Topological phase separation in a two-dimensional quantum lattice Bose-Hubbard system away from half-filling

A. S. Moskvin
Ural State University, 620083 Ekaterinburg, Russia
(Received 2 December 2003; revised manuscript received 5 April 2004; published 11 June 2004)

We suppose that the doping of the two-dimensional (2D) hard-core (hc) boson system away from half-filling may result in the formation of a multicenter topological inhomogeneity (defect), such as charge order (CO) bubble domain(s) with Bose superfluid (BS) and extra bosons both localized in domain wall(s), or else in a topological CO+BS phase separation rather than a uniform mixed CO+BS supersolid phase. Starting from the classical model, we predict the properties of the respective quantum system. The long-wavelength behavior of the system is believed to be reminiscent of that of granular superconductors, charge-density wave materials, Wigner crystals, and multi-Skyrmion systems akin to the quantum Hall ferromagnetic state of a 2D electron gas. To elucidate the role played by quantum effects and that of the lattice discreteness, we have addressed the simplest nanoscopic counterpart of the bubble domain in the checkerboard CO phase of a 2D hc Bose-Hubbard (BH) square lattice. It is shown that the relative magnitude and symmetry of a multicomponent order parameter are mainly determined by the sign of the nearest-neighbor and next-nearest-neighbor transfer integrals. In general, the topologically inhomogeneous phase of the hc-BH system away from the half-filling can exhibit the signatures of the *s*, *d*, and *p* symmetries of the off-diagonal order.

DOI: 10.1103/PhysRevB.69.214505 PACS number(s): 74.25.Dw, 05.30.Jp, 03.75.Lm

I. INTRODUCTION

The model of quantum lattice Bose gas has a long history and has been suggested initially for conventional superconductors,[1] quantum crystals such as ^{4}He where superfluidity coexists with a crystalline order.[2,3] Afterwards, the Bose-Hubbard (BH) model has been studied as a model of the superconductor-insulator transition in materials with local bosons, bipolarons, or preformed Cooper pairs.[4,5] Two-dimensional BH models have been addressed as relevant to describe the superconducting films and Josephson junction arrays. The most recent interest to the system of hard-core bosons comes from the delightful results on Bose-Einstein (BE) condensed atomic systems produced by trapping bosonic neutral atoms in an optical lattice.[6] The progress in boson physics generates an especial interest around nonlinear topological excitations (Skyrmions, vortices) which play an increasingly significant role in physics.

One of the fundamental hotly debated problems in bosonic physics concerns the evolution of the charge ordered (CO) ground state of the two-dimensional (2D) hard-core BH model (hc-BH) with a doping away from half-filling. Numerous model studies steadily confirmed the emergence of "supersolid" phases with simultaneous diagonal and off-diagonal long-range order, while Penrose and Onsager[7] showed as early as 1956 that supersolid phases do not occur. The most recent quantum Monte Carlo (QMC) simulations[8–10] found two significant features of the 2D Bose-Hubbard model with a screened Coulomb repulsion: the absence of the supersolid phase at half-filling, and a growing tendency to phase separation (CO+BS) upon doping away from half-filling. Moreover, Batrouni and Scalettar[8] studied quantum phase transitions in the ground state of the 2D hard-core boson Hubbard Hamiltonian and have shown numerically that, contrary to the generally held belief, the most commonly discussed "checkerboard" supersolid is thermodynamically unstable and phase separates into solid and superfluid phases. The physics of the CO+BS phase separation in the Bose-Hubbard model is associated with a rapid increase of the energy of a homogeneous CO state with doping away from half-filling due to a large "pseudo-spin-flip" energy cost. Hence, it appears to be energetically more favorable to "extract" extra bosons (holes) from the CO state and arrange them into finite clusters with a relatively small number of particles. Such a droplet scenario is believed to minimize the long-range Coulomb repulsion. However, immediately there arise several questions, such as can a simple mean-field approximation (MFA) and classical continuum model predict such a behavior? What is the detailed structure of the CO+BS phase-separated state? What are the main factors governing the essential low-energy and long-wavelength physics? Is it possible to make use of simple toy models? Are there analogies with the fermion Hubbard model? The behavior of the latter under doping away from half-filling is extensively studied in the last decade in the stripe scenario which implies that doping may proceed through the formation of stripes, or charged domain walls being specific topological solitons in Néel antiferromagnets. In particular, Emery and Kivelson[11] argued that the phase separation reflects a universal tendency of the correlated antiferromagnet to expel the doped holes. White and Scalapino[12] showed that the pure 2D *t-J* model, in the small-J/t regime, and with dopings near $x \sim 0.1$, has a striped ground state. In general, the topological phase separation is believed to be a generic property of the 2D fermion Hubbard model.

In the paper we present a topological scenario of CO+BS phase separation in the 2D hc-BH model with intersite repulsion. The extra bosons/holes doped to a checkerboard CO phase of the 2D boson system are believed to be con-

fined in the ring-shaped domain wall of the Skyrmion-like topological defect, which looks like a bubble domain in an easy-axis antiferromagnet. This allows us to propose the mechanism of 2D topological CO+BS phase separation when the doping of the bare checkerboard CO phase results in the formation of a multicenter topological defect, in which the simplified pseudospin pattern looks like a system of bubble CO domains with Bose superfluid confined in charged ring-shaped domain walls.

The rest of the paper is organized as follows. In Sec. II we give a short overview of the conventional hc-BH model in the frame of a pseudospin formalism and MFA description. In Sec. III we show that the doping in a 2D hc-BH system can be accompanied by the formation of a topological defect like a single or multicenter Skyrmion. We present the scenario of the essential low-energy physics for the topologically doped hc-BH system. In Sec. IV we address a simple model of a nanoscopic bubblelike domain in a checkerboard CO phase for a discrete square lattice that allows us to demonstrate the subtle microscopic structure of such a center with a multicomponent order parameter.

II. HARD-CORE BOSE-HUBBARD MODEL

A. Effective Hamiltonian and pseudospin formalism

The Hamiltonian of a hard-core Bose gas on a lattice can be written in a standard form as follows:

$$H_{BG} = -\sum_{i>j} t_{ij}\hat{P}(B_i^\dagger B_j + B_j^\dagger B_i)\hat{P} + \sum_{i>j} V_{ij}N_iN_j - \mu\sum_i N_i, \tag{1}$$

where $\hat{P}$ is the projection operator that removes the double occupancy of any site, $N_i=B_i^\dagger B_i$, and μ is the chemical potential determined from the condition of a fixed full number of bosons $N_l=\Sigma_{i=1}^N \langle N_i\rangle$ or concentration $n=N_l/N\in[0,1]$. The t_{ij} denotes an effective transfer integral and V_{ij} is an intersite interaction between the bosons. Here $B^\dagger(B)$ are the Pauli creation (annihilation) operators, which are commuting Bose-like for different sites $[B_i,B_j^\dagger]=0$, if $i\neq j$, $[B_i,B_i^\dagger]=1-2N_i$, $N_i=B_i^\dagger B_i$; N is a full number of sites. It is worth noting that near half-filling ($n\approx 1/2$) one might introduce the renormalization $N_i\to(N_i-1/2)$, or neutralizing background, that immediately provides the particle-hole symmetry.

The model of hard-core Bose gas with an intersite repulsion is equivalent to a system of spins $s=1/2$ exposed to an external magnetic field in the z direction. For the system with a neutralizing background we arrive at an effective pseudospin Hamiltonian

$$H_{BG} = \sum_{i>j} J_{ij}^{xy}(s_i^+s_j^- + s_j^+s_i^-) + \sum_{i>j} J_{ij}^z s_i^z s_j^z - \mu\sum_i s_i^z, \tag{2}$$

where $J_{ij}^{xy}=2t_{ij}$, $J_{ij}^z=V_{ij}$, $s^-=(1/\sqrt{2})B$, $s^+=-(1/\sqrt{2})B^\dagger$, $s^z=-(1/2)+B_i^\dagger B_i$, $s^\pm=\mp(1/\sqrt{2})(s^x\pm\imath s^y)$.

In a linear approximation the Hamiltonian for the coupling with an electromagnetic field reads as follows:

$$\hat{V}_{int} = \sum_{i<j}\hat{t}_{ij}\left((\Phi_j-\Phi_i)[\hat{\mathbf{s}}_i\times\hat{\mathbf{s}}_j]_z - \frac{1}{2}(\Phi_j-\Phi_i)^2(\hat{\mathbf{s}}_i\cdot\hat{\mathbf{s}}_j)\right), \tag{3}$$

$$(\Phi_j-\Phi_i) = -\frac{q}{\hbar c}\int_{\mathbf{R}_i}^{\mathbf{R}_j}\mathbf{A}(\mathbf{r})d\mathbf{r}, \tag{4}$$

where $\mathbf{A}$ is the vector potential, and integration runs over the line binding the i and j sites,

$$(\hat{\mathbf{s}}_i\cdot\hat{\mathbf{s}}_j) = \frac{1}{2}(\hat{B}_i^\dagger\hat{B}_j + \hat{B}_i\hat{B}_j^\dagger), \quad [\hat{\mathbf{s}}_i\times\hat{\mathbf{s}}_j]_z = \frac{i}{2}(\hat{B}_i^\dagger\hat{B}_j - \hat{B}_i\hat{B}_j^\dagger). \tag{5}$$

However, the pseudospins are assumed to lie in the xy plane. Then the boson current density operator may represent a sum of the paramagnetic

$$\mathbf{j}^p(\mathbf{R}_i) = \frac{q}{\hbar}\sum_j \hat{t}_{ij}\mathbf{R}_{ij}[\hat{\mathbf{s}}_i\times\hat{\mathbf{s}}_j]_z \tag{6}$$

and diamagnetic

$$\mathbf{j}^d(\mathbf{R}_i) = -\frac{q}{2\hbar}\sum_j \hat{t}_{ij}\mathbf{R}_{ij}(\Phi_j-\Phi_i)(\hat{\mathbf{s}}_i\cdot\hat{\mathbf{s}}_j) \tag{7}$$

terms, respectively.

B. Uniform phases: Mean-field approximation

Below we make use of a conventional two-sublattice MFA approach. For the description of the pseudospin ordering to be more physically clear, one may introduce two vectors, the ferromagnetic and antiferromagnetic ones,

$$\mathbf{m} = \frac{1}{2s}(\langle\mathbf{s}_1\rangle + \langle\mathbf{s}_2\rangle); \quad \mathbf{l} = \frac{1}{2s}(\langle\mathbf{s}_1\rangle - \langle\mathbf{s}_2\rangle); \quad \mathbf{m}^2+\mathbf{l}^2=1,$$

where $\mathbf{m}\cdot\mathbf{l}=0$. For the plane where these vectors lie, one may introduce a two-parametric angular description: $m_x=\sin\alpha\cos\beta$, $m_z=-\sin\alpha\sin\beta$, $l_x=\cos\alpha\sin\beta$, $l_z=\cos\alpha\cos\beta$. The hard-core boson system in a two-sublattice approximation is described by two diagonal order parameters l_z, m_z and two complex off-diagonal order parameters $m_\pm=\mp(1/\sqrt{2})(m_x\pm\imath m_y)$ and $l_\pm=\mp(1/\sqrt{2})(l_x\pm\imath l_y)$. The complex superfluid order parameter $\Psi(\mathbf{r})=|\Psi(\mathbf{r})|\exp(-\imath\varphi)$ is determined by the in-plane components of the ferromagnetic vector: $\Psi(\mathbf{r})=(1/2)\langle(\hat{B}_1+\hat{B}_2)\rangle=sm_-=sm_\perp\exp(-\imath\varphi)$, $m_\perp$ being the length of the in-plane component of the ferromagnetic vector. So, for a local condensate density we get $n_s=s^2m_\perp^2$. It is of interest to note that, in fact, all the conventional uniform $T=0$ states with nonzero $\Psi(\mathbf{r})$ imply a simultaneous long-range order both for modulus $|\Psi(\mathbf{r})|$ and phase φ. The in-plane components of the antiferromagnetic vector $l_\pm$ describe a staggered off-diagonal order. It is worth noting that by default, one usually considers the negative sign of the transfer integral t_{ij}, which implies the ferromagnetic in-plane pseudospin ordering.

The model exhibits many fascinating quantum phases and phase transitions. Early investigations predict at $T=0$, charge

order (CO), Bose superfluid (BS), and mixed (CO+BS) supersolid uniform phases with an Ising-type melting transition (CO-NO) and Kosterlitz-Thouless-type (BS-NO) phase transitions to a nonordered normal fluid (NO).[13] The detailed mean-field and spin-wave analysis of the uniform phases of 2D hc-BH model is given by Pich and Frey.[14] The MFA yields for the conventional uniform supersolid phase are[4]

$$\sin^2\beta = m_z\frac{\sqrt{V-2t}}{\sqrt{V+2t}}, \quad \sin^2\alpha = m_z\frac{\sqrt{V+2t}}{\sqrt{V-2t}}$$

with a constant chemical potential $\mu = 4s\sqrt{(V^2-4t^2)}$. It should be noted that the supersolid phase appears to be unstable with regard to small perturbations in the Hamiltonian. The mean-field energy per site of the uniform supersolid phase is written as follows:

$$E_{SS} = E_{CO} + s\mu m_z = E_{CO} + \mu\left(n_B - \frac{1}{2}\right),$$

where $E_{CO} = -2Vs^2$. The cost of doping both for the CO and CO+BS phase appears to be rather high as compared with an easy-plane BS phase at half-filling, where the chemical potential turns into zero.[15]

III. DOPING OF THE BH SYSTEM AWAY FROM HALF-FILLING: CONTINUOUS LIMIT

A. Topological phase separation: Skyrmion-like bubble domains

Magnetic analogy allows us to make unambiguous predictions regarding the doping of the BH system away from half-filling. Indeed, the boson/hole doping of the checkerboard CO phase corresponds to the magnetization of an antiferromagnet in the z direction. In the uniform easy-axis l_z phase of an anisotropic antiferromagnet the local spin-flip energy cost is rather big. In other words, the energy cost for boson/hole doping into the checkerboard CO phase appears to be big due to a large contribution of boson-boson repulsion. However, the magnetization of the anisotropic antiferromagnet in an easy-axis direction may proceed as a first order phase transition with a "topological phase separation" due to the existence of antiphase domains.[16] The antiphase domain walls provide the natural nucleation centers for a spin-flop phase having enhanced magnetic susceptibility as compared with small if any longitudinal susceptibility, thus providing the advantage of the field energy. Namely, domain walls would specify the inhomogeneous magnetization pattern for such an anisotropic easy-axis antiferromagnet in a relatively weak external magnetic field. As concerns the domain type in a quasi-two-dimensional antiferromagnet, one should emphasize the specific role played by the cylindrical, or bubble, domains which have finite energy and size. These topological solitons have the vortexlike in-plane spin structure and are often named "Skyrmions." The classical, or Belavin-Polyakov (BP) Skyrmion[17] describes the solutions of a nonlinear σ model with a classical isotropic 2D Heisenberg Hamiltonian, and represents one of the generic toy model spin textures. It is of primary importance to note that Skyrmion-like bubble domains in easy-axis layered antiferromagnets were actually observed in the experiments performed by Waldner,[18] which were supported later by different authors (see, e.g., Refs. 19 and 20). Although some questions were not completely clarified and remain open until now,[21,22] the classical and quantum[23,24] Skyrmion-like topological defects are believed to be a genuine element of essential physics both of ferro- and antiferromagnetic 2D easy-axis systems.

The magnetic analogy seems to be a little bit naive; however, it catches the essential physics of doping the hc-BH system. As regards the checkerboard CO phase of such a system, namely, a finite energy Skyrmion-like bubble domain[25] seems to be the most preferable candidate for the domain with the antiphase domain wall providing the natural reservoir for extra bosons. The classical description of nonlinear excitations in the hc-BH model includes the Skyrmionic solution given $V=2t$. [25] The Skyrmion spin texture consists of a vortexlike arrangement of the in-plane components of the ferromagnetic **m** vector with the l_z component reversed in the center of the Skyrmion and gradually increases to match the homogeneous background at infinity. The simplest spin distribution within the classical Skyrmion is given as follows:

$$m_x = m_\perp\cos(\varphi+\varphi_0), \quad m_y = m_\perp\sin(\varphi+\varphi_0),$$

$$m_\perp = \frac{2r\lambda}{r^2+\lambda^2}, \quad l_z = \frac{r^2-\lambda^2}{r^2+\lambda^2}, \tag{8}$$

where φ_0 is a global phase [$U(1)$ order parameter] and λ is the Skyrmion radius. The Skyrmion spin texture describes the coexistence and competition of the staggered charge order parameter l_z and the BS order parameter $m_\perp$ (see Fig. 1) that reflects a complex spatial interplay of potential and kinetic energies. The Skyrmion looks like a bubble domain in an easy-axis magnet. It should be noted that the domain wall in such a bubble domain somehow created in the checkerboard CO phase of the 2D hc-BH system represents an effective ring-shaped reservoir both for the Bose superfluid and the extra boson/hole. Indeed, the soliton energy depends quadratically on the number Δn of bosons bound in the domain wall,[25] similar to that of the homogeneous BS phase.[15] In other words, one might say this about a zero value of the effective boson/hole chemical potential for the CO bubble domain configuration, provided it was a ground state. The numerical calculations performed in the classical continuous model[26] show that the doped bosons appear to be trapped inside the bubble domain wall. The spatial distribution of the doped boson/hole density ($\propto m_z$) in the charged Skyrmion is shown schematically in Fig. 1(c).

Skyrmions are characterized by the magnitude and sign of its topological charge, by its size (radius), and by the global orientation of the spin. The scale invariance of the classical BP Skyrmionic solution reflects this, in that its energy does not depend on the radius and global phase. An interesting example of topological inhomogeneity is provided by a multicenter BP Skyrmion,[17] in which energy does not depend on

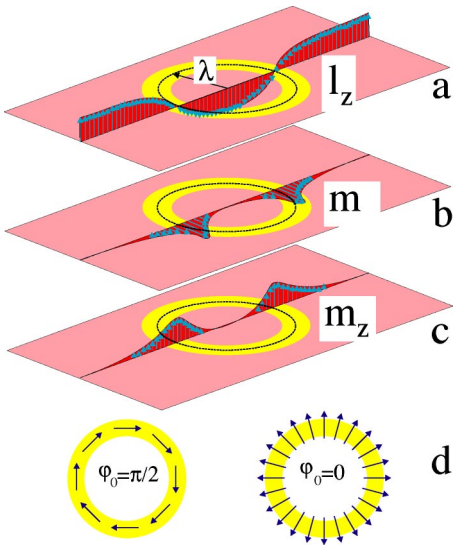

FIG. 1. The order parameters distribution in the Skyrmion: (a) The radial distribution of the staggered charge order parameter l_z; (b) the radial distribution of the modulus of the superfluid order parameter $\mathbf{m}_\perp$; (c) the radial distribution of the charge density $\mathbf{m}_z$ for the charged Skyrmion; (d) the orientation of the superfluid order parameter $\mathbf{m}_\perp$ given two values of the phase order parameter φ_0: $\varphi_0=0,\pi/2$, respectively. Rings in all the pictures correspond to the Skyrmion (bubble domain) wall, the dashed circle being its center.

the position of the centers. The latter are believed to be addressed as an additional degree of freedom, or positional order parameter.

In the continuous model, the classical BP Skyrmion is a topological excitation and cannot dissipate. However, the classical static Skyrmion is unstable with regard to an external field or anisotropic interactions, both of the easy-plane and easy-axis types. Small easy-axis anisotropy or an external field are sufficient to shrink the Skyrmion to a nanoscopic size when the magnetic length l_0,

$$l_0 = [\sqrt{(2V/t)^2 - (\mu/t)^2} - 4]^{-1/2},$$

is of the order of several lattice parameters, and the continuous approximation fails to correctly describe the excitations. Nonetheless, Abanov and Pokrovsky[27] have shown that the easy-axis anisotropy together with the fourth-order exchange term can stabilize the Skyrmion with radius $R \propto \sqrt{l_0}$.

B. Topological phase separation: Skyrmion lattices and the low-energy physics of the BH model away from half-filling

A Skyrmionic scenario in the hc-BH model allows us to make several important predictions. Away from half-filling one may anticipate the nucleation of a topological defect in the unconventional form of the multicenter Skyrmion-like object with ring-shaped Bose superfluid regions positioned in an antiphase domain wall, separating the CO core and the CO outside of the single Skyrmion. The specific spatial separation of BS and CO order parameters that avoid each other reflects the competition of kinetic and potential energy. Such a topological (CO+BS) phase separation is believed to provide a minimization of the total energy as compared with its uniform supersolid counterpart. Thus, the parent checkerboard CO phase may gradually lose its stability under boson/hole doping, while a topological self-organized texture is believed to become stable. The most probable possibility is that every domain wall accumulates a single boson, or boson hole. Then, the number of centers in a multicenter Skyrmion nucleated with doping has to be equal to the number of bosons/holes. In such a case, we anticipate the near-linear dependence of the total BS volume fraction on the doping. Generally speaking, one may assume the scenario where the nucleation of a multicenter Skyrmion occurs spontaneously with no doping. In such a case we should anticipate the existence of a neutral multicenter Skyrmion-like object with an equal number of positively and negatively charged single Skyrmions. However, in practice, namely the boson/hole doping is likely to be a physically clear driving force for a nucleation of a single, or multicenter Skyrmion-like self-organized collective mode in the form of a multicenter charged topological defect which may be (not strictly correctly) referred to as a multi-Skyrmion system akin to the quantum Hall ferromagnetic state of a two-dimensional electron gas.[28] In such a case, we may characterize an individual Skyrmion by its position (i.e., the center of Skyrmionic texture), its size (i.e., the radius of domain wall), and the orientation of the in-plane components of pseudospin [$U(1)$ degree of freedom]. An isolated Skyrmion is described by the inhomogeneous distribution of the CO parameter, or staggered boson density l_z, the order parameter m_z characterizing the deviation from the half-filling, and the $m_\perp$ that corresponds only to the modulus of the superfluid order parameter.

It seems likely that for a light doping, any doped particle (boson/holes) results in a nucleation of a new single-Skyrmion state, hence its density changes gradually with particle doping. Therefore, as long as the separation between Skyrmionic centers is sufficiently large so that the inter-Skyrmion interaction is negligible, the energy of the system per particle remains almost constant. This means that the chemical potential of a boson or hole remains unchanged with doping and hence apparently remains fixed.

The multi-Skyrmionic system, in contrast with the uniform ones, can form the structures with an inhomogeneous long-range ordering of the modulus of the superfluid order parameter, accompanied by the nonordered global phases of single Skyrmions. Such a situation resembles, in part, that of granular superconductivity.

In the long-wavelength limit, the off-diagonal ordering can be described by an effective Hamiltonian in terms of the $U(1)$ (phase) degree of freedom associated with each Skyrmion. Such a Hamiltonian contains a repulsive, long-range Coulomb part and a short-range contribution related to the phase degree of freedom. The latter term can be written out in the standard form for the XY model of a so-called Josephson coupling

$$H_J = -\sum_{\langle i,j \rangle} J_{ij} \cos(\varphi_i - \varphi_j), \tag{9}$$

where φ_i, φ_j are global phases for Skyrmions centered at points i and j, respectively, J_{ij} is the Josephson coupling

parameter. Namely, the Josephson coupling gives rise to the long-range ordering of the phase of the superfluid order parameter in a multicenter Skyrmion. Such a Hamiltonian represents a starting point for the analysis of disordered superconductors, granular superconductivity, and an insulator-superconductor transition with an $\langle i,j\rangle$ array of superconducting islands with phases φ_i, φ_j. Calculating the phase-dependent part of Skyrmion-Skyrmion interaction, Timm *et al.*[29] arrived at a *negative* sign of J_{ij} that favors antiparallel alignment of the $U(1)$ pseudospins. In other words, two Skyrmions are believed to form a peculiar Josephson π microjunction. There are a number of interesting implications that follow directly from this result:[30] the spontaneous breaking of time-reversal symmetry with nonzero supercurrents and magnetic fluxes in the ground state, the long-time tails in the dynamics of the system, the unconventional Aharonov-Bohm period $hc/4e$, and negative magnetoresistence.

To account for Coulomb interaction and to allow for quantum corrections, we should introduce into the effective Hamiltonian the charging energy[30]

$$H_{ch} = -\frac{1}{2}q^2\sum_{i,j} n_i(C^{-1})_{ij}n_j,$$

where n_i is a boson number operator for bosons bound in the ith Skyrmion; it is quantum-mechanically conjugated to $\varphi: n_i = -i\partial/\partial\varphi_i$, $(C^{-1})_{ij}$ stands for the capacitance matrix, q for bosonic charge.

The classical ground-state energy of the Skyrmion lattice for all reasonable two-dimensional lattice structures was minimized by Timm *et al.* taking the $U(1)$ order into account.[29] Besides the expected triangular lattice with frustrated antiferromagnetic $U(1)$ order and the square lattice with Néel $U(1)$ order, the authors have also obtained ground-state energies for all 2D Bravais lattices. Such a system appears to reveal a tremendously rich quantum-critical structure. In the absence of disorder, the $T=0$ phase diagram of the multi-Skyrmion system implies either triangular or square crystalline arrangements (Skyrmion, or bubble crystal) with a possible melting transition to a Skyrmion (bubble) liquid (see Fig. 2). The melting of the Skyrmion lattice is successfully described by applying the Berezinsky-Kosterlitz-Thouless (BKT) theory to dislocations and disclinations of the lattice and it proceeds in two steps. The first implies the transition to a liquid-crystal phase with short-range translational order, the second does the transition to isotropic liquid. Disorder pins the Skyrmion lattice and also causes the crystalline order to have a finite correlation length. For such a system, provided the Skyrmion positions are fixed at all temperatures, the long-wavelength physics would be described by an *XY* model with an expectable BKT transition and a gapless *XY* spin-wave mode.

The classical phase diagram of the Skyrmion lattice is quite rich. Depending on the relation between Coulomb and Josephson coupling and density one may arrive at different lattice structures with continuous or first-order phase transitions. As regards the superfluid properties, the Skyrmionic system reveals unconventional behavior with two critical

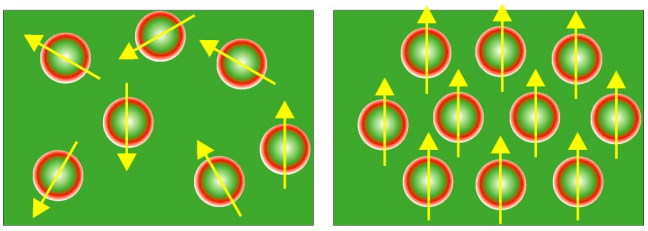

FIG. 2. Bubble textures for the bubble liquid and bubble crystal. The arrows show the global phase order parameter. The left-hand side panel shows a snapshot of the bubble texture in liquid state with nonordered global phase. The right-hand-side panel illustrates the triangular bubble crystal state with a "ferromagnetically" ordered global phase. Rings in all the pictures correspond to the bubble domain wall.

temperatures $T_{BS} \leqslant t$ and $T_c \leqslant J$, T_{BS} being the temperature of the ordering of the modulus and $T_c < T_{BS}$, that of the phase of order parameter Ψ. The low-temperature physics in Skyrmion crystals is governed by an interplay of two BKT transitions, for the $U(1)$ phase and for positional degrees of freedom, respectively.[29] Dislocations in most Skyrmion lattice types lead to a mismatch in the $U(1)$ degree of freedom, which makes the dislocations bind fractional vortices and lead to a coupling of translational and phase excitations. Both BKT temperatures either coincide (square lattice) or the melting one is higher (triangular lattice).[29] Quantum fluctuations can substantially affect these results. Quantum melting can destroy $U(1)$ order at sufficiently low densities, where the Josephson coupling becomes exponentially small. A similar situation is expected to take place in the vicinity of structural transitions in a Skyrmion crystal. With the increasing of the Skyrmion density, the quantum effects result in a significant lowering of the melting temperature as compared with classical square-root dependence. The resulting melting temperature can reveal an oscillating behavior as a function of particle density with zeros at the critical (magic) densities associated with structural phase transitions.

In terms of our model, the positional order corresponds to an incommensurate charge density wave, while the $U(1)$ order does so to a superconductivity. In other words, we arrive at a subtle interplay between two orders. The superconducting state evolves from a charge order with $T_C \leqslant T_m$, where T_m is the temperature of a melting transition that could be termed as a temperature of the opening of the insulating gap (pseudogap?).

The normal modes of a dilute Skyrmion system (multicenter Skyrmion) include the pseudospin waves propagating in between the Skyrmions, the positional fluctuations, or phonon modes of the Skyrmions, which are gapless in a pure system, but gapped when the lattice is pinned, and, finally, fluctuations in the Skyrmionic in-plane orientation and size. The latter two types of fluctuation are intimitely connected, since the z component of the spin and the orientation are conjugate coordinates because of commutation relations of quantum angular momentum operators. So, rotating a Skyr-

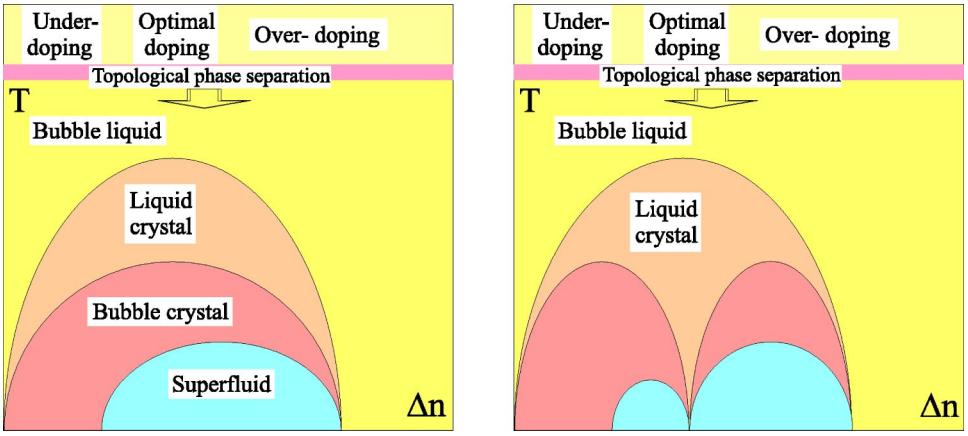

FIG. 3. The low-temperature part of the schematical Δn-T phase diagram for the hc-BH model with topological phase separation. The gradual Skyrmionic solidifications evolves from the isotropic Skyrmion (bubble) liquid phase, the Skyrmion liquid-crystal phase, the incommensurate Skyrmion crystal phase, and $U(1)$ ordering, or the superfluid phase, restricted by the temperatures of the proper BKT transitions. The right-hand-side panel differs by the assumed structural phase transition in the bubble lattice at a magic doping such as $\Delta n_b = 1/16$.

mion changes its size. The orientational fluctuations of the multi-Skyrmion system are governed by the gapless XY model.[28] The relevant model description is most familiar as an effective theory of the Josephson junction array. An important feature of the model is that it displays a quantum-critical point.

The low-energy collective excitations of Skyrmion liquid includes a usual longitudinal acoustic phonon branch. The liquid crystal phases differ from the isotropic liquid in that they have massive topological excitations, i.e., the disclinations. One should note that the liquids do not support transverse modes, these could survive in a liquid state only as overdamped modes. Therefore, it is reasonable to assume that solidification of the Skyrmion lattice would be accompanied by a stabilization of transverse modes with its sharpening below the melting transition. In other words, an instability of transverse phonon modes signals the onset of melting. A generic property of the positionally ordered Skyrmion configuration is the sliding mode, which is usually pinned by the disorder. The depinning of sliding mode(s) can be detected in a low-frequency and low-temperature optical response.

C. Implications for the "doping-temperature" phase diagram of a hc-BH model

Our speculations with regard to the topological phase separation and long-wavelength physics of the 2D hc-BH model are summarized in a qualitative Δn-T ($\Delta n_b = n_b - 0.5$) phase diagram in Fig. 3. First of all, the phase diagram implies a scenario in which the topological phase separation state evolves with minimal doping, though it is worth noting that the ideal checkerboard CO phase cannot be a nominal $\Delta n_b = 0$ limit of any topologically phase-separated phase.

Despite the qualitative character of the phase diagram we took into account some quantitative results of quantum Monte Carlo calculations for the 2D hc-BH model with nearest-neighbor Coulomb repulsion.[8,10] First, it concerns the doping range of the additive, or near-linear concentration behavior of the Bose-condensate density ρ_s and the CO structure factor $S(\mathbf{q})$. The superfluid density increases approximately linearly with the doping except for the most overdoped point $\Delta n_b \approx 0.1$, where it turns down again. Diagonal long-range charge order is characterized by the equal time structure factor at the ordering vector $\mathbf{q}$,

$$S(\mathbf{q}) = \frac{1}{N}\sum_{\mathbf{l}} e^{i\mathbf{q}\cdot\mathbf{l}}\langle n(\mathbf{j},\tau)n(\mathbf{j}+\mathbf{l},\tau)\rangle. \tag{10}$$

In the presence of long-range order, $S(\mathbf{q})$ will diverge with the system size $S(\mathbf{q}) \propto L^2$ for a given ordering momentum $\mathbf{Q}$, which characterizes the ordered phase. For the checkerboard order $\mathbf{Q} = (\pi, \pi)$. In the concentration range $\Delta n_b = 0.0 - 0.1$, where both quantities vary linearly with Δn_b,[8] we may approximate the topological defect to be a system of $\Delta N = N\Delta n_b$ interacting single-charged Skyrmions. It should be noted that both the CO and BS order parameters coexist in a rather narrow doping concentration interval: $\Delta n_b \leqslant 0.11$. Beyond this "overdoping" region we deal with an inhomogeneous boson liquid whose pseudospin picture implies a strongly frustrated singlet-triplet system that resembles the spin glass, and may be termed as a dynamical "singlet-triplet" pseudospin glass. Such a system can be characterized by a dynamical short-range diagonal and off-diagonal ordering with a wide distribution of respective correlation lengths and relaxation rates. Interestingly, in the frame of a continuous model this phase is still described to be a strongly correlated multicenter topological defect. However, such a model obviously fails to describe the real system where the intercenter spacing is comparable with the lattice parameter.

The temperature evolution of the hc-BH system with large intersite boson repulsion implies that the highest critical temperature $T_{CO}(\Delta n)$ separates the high-temperature nonordered (NO) phase (boson liquid) and a low-temperature quasi-CO phase with a disordered system of Skyrmions. The next critical temperature $T_{TPS}(\Delta n) \leqslant t$ points to the first-order phase

transition with a formation of the inhomogeneous Bose condensate in a single Skyrmion with the vortexlike texture of the quasilocal order parameter $\mathbf{m}_{\perp}$. In other words, it is a temperature of the topological CO+BS phase separation (TPS). In frames of our scenario such a TPS state emerges with a minimal doping, and $T_{TPS}(\Delta n_b)$ is likely to be nearly constant in a linear doping regime ($\Delta n_b = 0.0-0.1$). The low-temperature part of the phase diagram, which is schematically shown in Fig. 3, describes the gradual Skyrmionic solidification and may include the isotropic Skyrmion (bubble) liquid phase, the Skyrmion liquid-crystal phase, the incommensurate Skyrmion crystal phase, and $U(1)$ ordering, or superfluid phase, restricted by the temperatures of the proper BKT transitions. For a small deviation from the half-filling ("underdoping") the temperatures of bubble crystallization/melting seemingly obey the square root concentration law $T_m \propto \sqrt{\Delta n_b}$ with a strongly developed quantum melting effect when approaching an "overdoped" regime or concentrations limiting the linear regime. The superfluid phase in Fig. 3 is arbitrarily chosen to lie inside the Skyrmion solid phase. One should emphasize the specific role played by quantum fluctuations: these lead to the melting of the bubble crystal at high densities and orientational disordering[29,31] at low densities. Both effects are of primary importance in the overdoped and the heavily underdoped regions of the phase diagram, respectively. Moreover, the quantum melting effect may strongly affect the phase diagram near the "magic" doping level, where the Skyrmion lattice undergoes the structural phase transition. For illustration, in the right-hand-side panel in Fig. 3 we present the possible phase diagram for a hc-BH system with a quantum melting effect near the "magic" doping level $\Delta n_b = 1/16$. In all cases, the critical doping level for the superfluid formation is determined by the magnitude of the Josephson coupling constant. It is worth noting that the bubble crystallization is accompanied by different (pseudo)gap effects.

Our interpretation of the phase transition at T_{TPS} differs from that in Ref. 10. This temperature is governed by the magnitude of the transfer integral, and believed to be a temperature of the emergence of the nonzero magnitude of the modulus of the superconducting order parameter rather than a critical temperature for an insulator to a superconductor transition as it is stated in Ref. 10. This conclusion seems to be a result of finite size effects and boundary conditions in QMC calculations, despite the authors' use of the most efficient QMC strategy. Such problems seem to be typical for a finite-size simulation of many phase transitions. In addition, we should note that MC calculations need a substantial increase in lattice size to reproduce quantitatively the long-wavelength physics because the size of the Skyrmion and the Skyrmion lattice parameter appear to be new characteristic lengths.

A close inspection of the phase diagram in Fig. 3, where $T_c \leqslant T_m < T_{TPS}$, does not provide optimistic expectations with regard to the high-temperature superconductivity in 2D hc-BH systems, even if the magnitude of the local boson transfer integral were as large as $t \approx 1000$ K. Nevertheless, the attractively large temperatures T_{TPS} of the topological phase separation, with the emergence of a nonzero local condensate density, engender different reasonable speculations with regard to its practical realization.

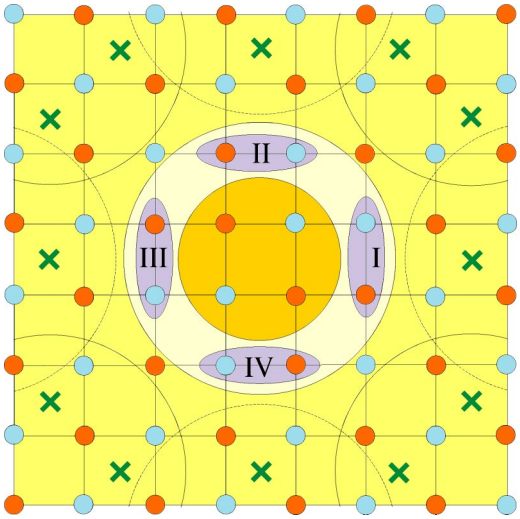

FIG. 4. Illustration for a Skyrmion-like bubble domain in a checkerboard CO phase with an eight-site ring-shaped domain wall. The four dimers within the domain wall are marked by I–IV. Schematically shown are nearest- and next-nearest-neighbor domains, which do not overlap with the central domain. It is worth noting that there are eight additional domains with strong nearest-neighbor interdimer coupling with the central domain. The centers of all 12 nearest-neighbor domains which do not overlap with the central domain are marked by crosses.

IV. TOPOLOGICAL PHASE SEPARATION IN DISCRETE LATTICES

Making use of the mean-field approximation together with simplified classical continuous models can hardly provide the quantitative description of a quantum lattice boson system. Both quantum effects and the discreteness of the Skyrmion texture can result in substantial deviations from the predictions of a classical model. The continuous model is relevant for discrete lattices only if we deal with long-wavelength inhomogeneities when their size is much bigger than the lattice spacing. In the discrete lattice the very notion of topological excitation seems to be inconsistent. At the same time, the discreteness of the lattice itself does not prohibit it from considering the nanoscale (pseudo)spin textures whose topology and spin arrangement is that of a Skyrmion.[32] Naturally, the typical continuous models fail to describe properly such short-wavelength nanoscopic inhomogeneities. Hereafter, we discuss a simple model which seems to catch the main effects of discreteness and quantization.

A. Nanoscopic bubble domain in a checkerboard CO phase

What is the lattice counterpart of the small Skyrmion-like bubble domain? Figure 4 presents the schematic view of the smallest Skyrmion-like bubble domain in a checkerboard CO phase for a 2D square lattice with an effective size of four lattice spacings. The domain wall is believed to include as a minimum eight sites forming a ring-shaped system of four dimers each composed of two sites. There are two types of such domains which differ by a rotation of $\pm\pi/2$. The for-

mation of such a center seems not to require a high energy. Indeed, the simple estimate of a change in potential energy, $\Delta V \approx 4\ V_{NN} - 6\ V_{NNN}$, points to a near cancelation of nearest-neighbor (NN) and next-nearest-neighbor (NNN) contributions. The remarkable feature of the domain is in a rather small magnitude both of scalar potential and electric field inside the eight-site domain wall (see Fig. 4). The flip energy for the dimer dipole moment is estimated to be $\delta V \approx V_{NN} - 2\ V_{NNN}$, compared with that for a bare checkerboard CO phase ($\delta V_0 \approx 3\ V_{NN} - 4\ V_{NNN}$) that implies rather subtle competition between NN and NNN couplings. However, the difference $(\delta V_0 - \delta V) = 2(V_{NN} - V_{NNN})$ is believed to be always positive and large. In other words, the flip energy for the dimer dipole may be relatively small. Respective dipole fluctuations would result in an effective screening of electrostatic repulsion energy, thus providing the stabilization of a bubblelike defect. An important additional mechanism of the domain stabilization in the hc-BH systems with local bosons composed from electron pairs may arise from the electron and lattice polarization effects.[33,34] As is well known, the respective energies are comparable in value with the intersite Coulomb interaction. Probably, namely both these effects might strongly contribute to the domain stabilization energy. On the other hand, the bubble geometry implies the formation of the electrostatic potential well inside the domain wall both for positive and negative charges. It means that the doping into a domain wall stabilizes the domain configuration. Such a doping may be energy costless, while the energy cost of the pseudospin flip in a checkerboard CO phase is rather high: $\Delta V \approx 4\ V_{NN} - 4\ V_{NNN}$, if the neutralizing background is taken into account.

B. Pseudospin formalism in a two-center dimer

Taking into account the kinetic energy (quantum tunneling) only inside the eight-site domain wall, we shall consider it as a quantum system in an external electrostatic potential field, assuming a rigid checkerboard CO ordering overall beyond the domain wall. Further, taking into account the reasonable relation: $|t_{NN}| \gg |t_{NNN}|$, we shall consider the domain wall to be a system of four dimers, or pairs of nearest-neighboring sites forming a quantum cluster. We anticipate that the model, though being simplified, would be very instructive in analyzing the role played both by quantum and discreteness effects.

Let us first address a simple two-site, or a dimer, system. The effective pseudospin Hamiltonian for such a cluster, or a single dimer Hamiltonian, can be written as follows:

$$\hat{H}_d = -t_{NN}\left[S(S+1) - \frac{3}{2}\right] + D\hat{S}_z^2 - h_S\,\hat{S}_z - h_T\,\hat{T}_z, \quad (11)$$

where $\hat{\mathbf{S}} = \hat{\mathbf{s}}_1 + \hat{\mathbf{s}}_2$ is the total pseudospin momentum, $\hat{\mathbf{T}} = \hat{\mathbf{s}}_1 - \hat{\mathbf{s}}_2$ is an operator that changes pseudospin multiplicity, $D = (1/2)V_{NN} + t_{NN}$, $h_S = \mu$, $h_T = (1/2)(V_{NN} - V_{NNN})$. The first two terms in this effective pseudospin Hamiltonian describe the intradimer interactions, while the last two describe its coupling with the off-domain-wall surroundings. It is worth noting that the condition $h_S = \mu$ means that the effective magnetic field produced by these surroundings turns into a zero

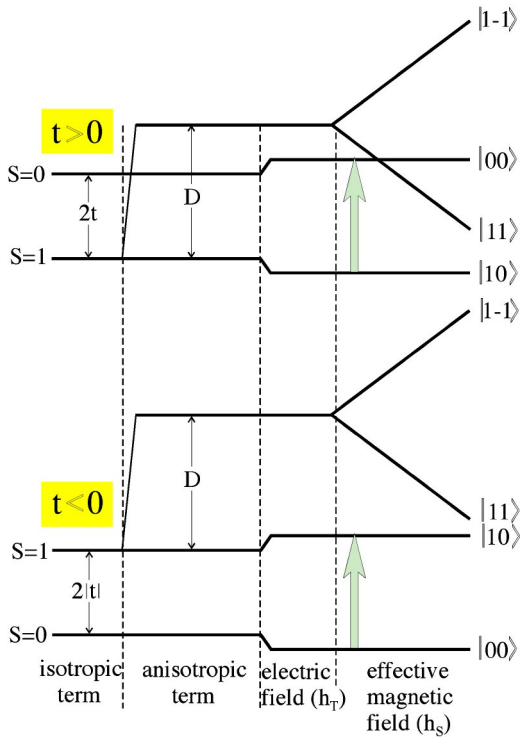

FIG. 5. The step-by-step formation of the dimer energy spectrum given different signs of the NN transfer integral. The arrows mark the dipole-allowed transitions (see text for details).

that provides the particle-hole symmetry of the dimer physics, in particular, for the domain wall doping. Actually, we arrive at an effective singlet-triplet model.[35] Both $\hat{\mathbf{S}}$ and $\hat{\mathbf{T}}$ operators have a rather simple physical sense: the former corresponds to the total "quantum" charge of the dimer, while the latter does to the total "quantum" dipole moment. Strictly speaking, the diagonal order parameters $\langle \hat{S}_z \rangle$ and $\langle \hat{T}_z \rangle$ describe the charge and dipole density, while the off-diagonal order parameters $\langle \hat{S}_\pm \rangle$ and $\langle \hat{T}_\pm \rangle$ describe the corresponding phase ordering. It is of primary importance to note that these order parameters are not independent because the respective operators obey the kinematic constraint,

$$\hat{\mathbf{S}}^2 + \hat{\mathbf{T}}^2 = 3; \quad (\hat{\mathbf{S}} \cdot \hat{\mathbf{T}}) = 0,$$

which stemmed from a simple spin algebra. It should be noted that there are two operators: $\hat{\mathbf{T}} = \mathbf{s}_1 - \mathbf{s}_2$ and $\hat{\mathbf{J}} = [\mathbf{s}_1 \times \mathbf{s}_2]$ that change the pseudospin multiplicity with their matrices being symmetric and antisymmetric, respectively,

$$\langle 00|T_z|10\rangle = \langle 10|T_z|00\rangle = 1,$$

$$\langle 00|J_z|10\rangle = -\langle 10|J_z|00\rangle = i.$$

The Hamiltonian (11) points to the competition of S and T orders in the ring-shaped domain wall.

Figure 5 shows a step-by-step formation of the energy spectrum of such a two-site cluster, or dimer. The arrows mark the dipole-allowed transitions that could be revealed in optical spectra. The tunnel states $|00\rangle$ and $|10\rangle$ describing

purely "half-filled" dimer states are mixed due to the electric field with the mixing level governed by the ratio $|h_T/2t_{NN}|$. If $|h_T| \gg 2|t_{NN}|$, we arrive at classical Néel-like "up-and-down" dimer state.

Hereafter, to describe our singlet-triplet quantum pseudospin system we start with trial functions

$$\psi = c_0\psi_{00} + \sum_j (a_j + ib_j)\psi_j, \tag{12}$$

where the spin functions $|1M\rangle$ in Cartesian basis are used: $\psi_z = |10\rangle$ and $\psi_{x,y} \sim (|11\rangle \pm |1-1\rangle)/\sqrt{2}$. The conventional spin operator is represented on this basis by a simple matrix

$$\langle \psi_i | S_j | \psi_k \rangle = -i\varepsilon_{ijk},$$

and for the order parameters one easily obtains

$$\langle \hat{\mathbf{S}} \rangle = -2[\mathbf{a} \times \mathbf{b}], \quad \langle \{\hat{S}_i \hat{S}_j\} \rangle = 2(\delta_{ij} - a_i a_j - b_i b_j) \tag{13}$$

given the normalization constraint $|c_0|^2 + \mathbf{a}^2 + \mathbf{b}^2 = 1$. Thus, for the case of the spin-1 system, the order parameters are determined by two classical vectors [two real components of one complex vector $\mathbf{c} = \mathbf{a} + i\mathbf{b}$ from Eq. (12)]. The two vectors are coupled, so the minimal number of dynamic variables describing the $S=1$ spin system appears to be equal to 4. For the dimer as the singlet-triplet center we have additional unconventional T,J-order parameters. For the respective averages we can easily obtain

$$\langle \hat{\mathbf{T}} \rangle = c_0^* \mathbf{c} + c_0 \mathbf{c}^*; \quad \langle \hat{\mathbf{J}} \rangle = i(c_0^* \mathbf{c} - c_0 \mathbf{c}^*).$$

Given the real value of the c_0 parameter we arrive at a simple form: $\langle \hat{\mathbf{T}} \rangle = 2c_0\mathbf{a}$, and $\langle \hat{\mathbf{J}} \rangle = -2c_0\mathbf{b}$.

C. Pseudospin formalism and MFA description of the domain wall

Now we may proceed with the interdimer coupling in the domain wall. Introducing the symmetrized superpositions of S and T vectors, we can write the pseudospin Hamiltonian of the interdimer interaction as follows:

$$\hat{H}_{dd} = \frac{1}{2} t_{NNN} \{ \mathbf{S}^2(a_{1g}) - \mathbf{S}^2(b_{1g}) + [\mathbf{S}(e_u)\mathbf{T}(e_u)] + \mathbf{T}^2(b_{2g}) - \mathbf{T}^2(b'_{2g}) \} + \frac{1}{2}(V_{NNN} - t_{NNN}) \{ S_z^2(a_{1g}) - S_z^2(b_{1g}) + [S_z(e_u)T_z(e_u)] + T_z^2(b_{2g}) - T_z^2(b'_{2g}) \}, \tag{14}$$

where

$$\mathbf{S}(a_{1g}) = (\mathbf{S}_I + \mathbf{S}_{II} + \mathbf{S}_{III} + \mathbf{S}_{IV}),$$

$$\mathbf{S}(b_{1g}) = (\mathbf{S}_I - \mathbf{S}_{II} + \mathbf{S}_{III} - \mathbf{S}_{IV}),$$

$$\mathbf{S}(e_u x) = (\mathbf{S}_I + \mathbf{S}_{II} - \mathbf{S}_{III} - \mathbf{S}_{IV}),$$

$$\mathbf{S}(e_u y) = (-\mathbf{S}_I + \mathbf{S}_{II} + \mathbf{S}_{III} - \mathbf{S}_{IV}),$$

$$\mathbf{T}(b_{2g}) = (\mathbf{T}_I + \mathbf{T}_{II} - \mathbf{T}_{III} - \mathbf{T}_{IV}),$$

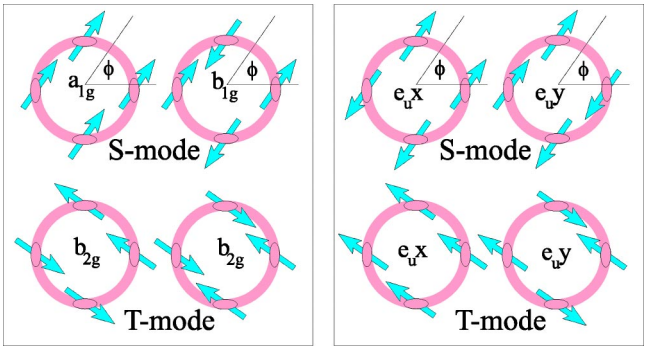

FIG. 6. Pseudospin orientation in different symmetry superpositions for the S and T order. Only the in-plane pseudospin components are shown.

$$\mathbf{T}(b'_{2g}) = (\mathbf{T}_I - \mathbf{T}_{II} - \mathbf{T}_{III} + \mathbf{T}_{IV}),$$

$$\mathbf{T}(e_u x) = (\mathbf{T}_I + \mathbf{T}_{II} + \mathbf{T}_{III} + \mathbf{T}_{IV}),$$

$$\mathbf{T}(e_u y) = (\mathbf{T}_I - \mathbf{T}_{II} + \mathbf{T}_{III} - \mathbf{T}_{IV})$$

(see Fig. 6). The chemical potential μ for the system of four dimers in a domain wall is determined now by the condition $\Sigma_{i=1}^4 \langle S_i^z \rangle = 0, \pm 1$ for the undoped and the singly doped (boson/hole) domain wall, respectively.

The respective mean values we can address as order parameters that describe the subtle structure of a domain wall with regard to the diagonal order, $\langle S_z(a_{1g}) \rangle$ specifies the full charge, $\langle S_z(e_u) \rangle$ and $\langle T_z(e_u) \rangle$ do the electric dipole moments, $\langle S_z(b_{1g}) \rangle$ the component of the quadrupole momentum, and one might introduce the higher order multipole moments. With regard to the off-diagonal order we should, in general, proceed with the three types (a_{1g}, e_u, b_{1g}, or s, p, d) of the S order, and three types [$e_u, b_{2g}(b'_{2g})$, or p, d] of the T order, which can be defined as follows:

$$\langle \hat{S}_-(\gamma) \rangle = \rho_\gamma^S e^{i\varphi_\gamma}, \quad \langle \hat{T}_-(\gamma) \rangle = \rho_\gamma^T e^{i\phi_\gamma}. \tag{15}$$

It is noteworthy to mention the kinematic constraint that couples different order parameters. In the absence of an external magnetic field, the energy does not depend on the **b** vector, it is restricted only to lie in the xy plane. In other words, we deal with the uncertainty of the J order parameter.

The mean-field domain-wall ground state corresponds to the coexistent $\mathbf{S}(a_{1g}), \mathbf{T}(b_{2g})$ modes given the negative sign of the transfer integral t_{NNN} or $\mathbf{S}(b_{1g}), \mathbf{T}(b'_{2g})$ modes given the positive sign of the transfer integral t_{NNN}. The relation between the S- and T-mode weight is specified by the relationship between the NN transfer integral t_{NN} and electric field h_T. If we assume $h_T = 0$, then given $t_{NN} > 0$, the dimers have a purely $S=1$ ground state, and we arrive at S-type off-diagonal order. In contrast, given $t_{NN} < 0$, we arrive at T type off-diagonal order. In general, neglecting the ST-mixing term leads to two independent phase order parameters. Generally speaking, the interference dipole-dipole ST term would result in ST mixing accompanied by the constraint on the phase order parameters with an appearance of a noncollinearity effect. Thus, we arrive at the conclusion that the symme-

try of the order parameter distribution in the domain wall would be specified only by the sign of the transfer integral. In addition, we see that the problem of the order parameter associated with our bubble domain is much more complicated than in a conventional BCS-like approach[36] due to its multicomponent nature. Moreover, we deal with a system with different symmetries of low-lying excited states and competing order parameters, which implies their possible ambiguous manifestation in either properties. The low-symmetry crystalline electric fields or crystal distortions would result in a mixing of the order parameters with different symmetry. The bubble domain (Fig. 4) yields a simple and instructive toy model to describe such effects.

It is worth noting that the flux quantization effects for the bubble domain, in particular the localizing effect of the magnetic field on the moving bosons, are expected to be observed only for rather large fields. Indeed, nanoscopic atomic systems such as a square plaquette with a size of around 10 Å, require a field of $H \approx 10^2$ T for a half-flux quantum per plaquette.

Above we are concerned with a simple one-center topological defect. However, in general one has to make use of a more complicated topological excitation like a multicenter BP Skyrmion.[17] The question arises as to whether such an entity may be described as a system of weakly coupled individual one-center defects. In practice, it seems to be a rather reasonable approach only for a slight deviation from half-filling, when the mean separation between doped particles is much larger than the effective domain size. The bubble domain may be called well isolated only if its environment does not contain another domain(s) which could be involved in a "dangerous" nearest-neighbor interdimer coupling. Each domain in Fig. 4 has $z=12$ of such neighbors. Hence the concentration of well-isolated domains can be written as follows: $P_0(x)=x(1-x)^z$, where z is a number of "dangerous" neighbors, and $x=\Delta n_b$ is the boson concentration. The $P_0(x)$ maximum is reached at $x_0=1/(z+1)$. In our case $x_0=1/13$, or ≈ 0.077. With increasing doping, the deviation of $P_0(x)$ from the linear law rises. On the other hand, knowing the effective domain area $S_d \approx 9a^2$ we can roughly estimate the limiting concentration of the single-domain model description to be $x_{max} \approx 1/9$ or 0.11. The interdomain coupling includes both long-range *SS* and short-range *TT* terms. We should emphasize a strong anisotropy of this coupling. For nearest neighbors along the [1,0] and [0,1] directions, the short-range (dipole-dipole) *TT* coupling would result in an effective suppression of the main *S* ordering (see Fig. 4), in contrast with the [11] direction.

Thus, we may conclude that the above-mentioned simple continuous model for Josephson junction arrays should be strongly modified to describe the multidomain configurations in 2D quantum hc-BH lattices, both with regard to the subtle internal domain structure, the competition of different order parameter, and the anisotropy of Josephson coupling.

V. CONCLUSIONS

The boson/hole doping of the hard-core boson system away from half-filling is assumed to be a driving force for the nucleation of a multicenter Skyrmion-like self-organized collective mode that resembles a system of CO bubble domains with a Bose superfluid and extra bosons both confined in domain walls. Such a topological CO+BS phase separation, rather than a uniform mixed CO+BS supersolid phase is believed to describe the evolution of the hc-BH model away from half-filling. Starting from the classical model we predict the properties of the respective quantum system. In our scenario we may anticipate, for the hc-BH model, the emergence of an inhomogeneous BS condensate for superhigh temperatures $T_{TPS} \leqslant t$, and three-dimensional superconductivity for rather high temperatures $T_c \leqslant J < t$. The system is believed to reveal many properties typical for granular superconductors, CDW materials, Wigner crystals, and multi-Skyrmion systems akin to the quantum Hall ferromagnetic state of a 2D electron gas. Topological inhomogeneity is believed to be a generic property of 2D hard-core boson systems away from half-filling. Such a behavior represents a boson counterpart of the so-called topological doping which is a general feature of Mott insulators or 2D fermion Hubbard models.[11]

Despite all shortcomings, the MFA and the continuous approximation are expected to provide a physically clear semiquantitative picture of rather complex transformations taking place in a bare CO system with doping, and can be instructive as a starting point to analyze possible scenarios. First of all, the MFA analysis allows us to consider the antiphase domain wall in the CO phase to be a very efficient ring-shaped potential well for the localization of a single extra boson (hole), thus forming a type of topological defect with a single-charged domain wall. Such a defect can be addressed as a charged Skyrmion-like quasiparticle whose energy can be approximated by its classical value for the CO bubble domain. It is of great importance to note that the domain wall simultaneously represents a ring-shaped reservoir for Bose superfluid.

Unfortunately, we have no experience dealing with multicenter Skyrmions with regard to structure, energetics, and stability. It should be noted that such a texture, with strongly polarizable centers, is believed to provide an effective screening of long-range boson-boson repulsion, thus resulting in an additional self-stabilization. Nucleation of the topological phase is likely to proceed in the way that is typical for the first-order phase transitions.

The role played by quantum effects and lattice discreteness has been illustrated as the simplest nanoscopic counterpart of the bubble domain in a checkerboard CO phase of the 2D hc-BH square lattice. It is shown that the relative magnitude and symmetry of the multicomponent order parameter are mainly determined by the sign of the NN and NNN transfer integrals. The topologically inhomogeneous phase of the hc-BH system away from the half-filling can exhibit the signatures both of the s, d, and p symmetry of the off-diagonal order. The model allows us to study the subtle microscopic details of the order parameter distribution, including its symmetry in a real, rather than momentum, space, though the problem of the structure and stability of nanoscale domain configurations remains to be solved. The present paper establishes only the framework for analyzing the subtleties of the phase separation in a lattice hc-BH model away from half-

filling. Much work remains to be done both in macroscopic and microscopic approaches.

ACKNOWLEDGMENTS

Stimulating discussions with C. Timm, S.-L. Drechsler, and T. Mishonov are acknowledged, and also support by the SMWK Grant, the INTAS Grant No. 01-0654, the CRDF Grant No. REC-005, the RME Grant Nos. E 02-3.4-392 and UR.01.01.062, and RFBR Grant No. 04-02-96077. I would also like to thank the Leibniz-Institut für Festkörper- und Werkstoffforschung Dresden, where part of this work was made, for hospitality.

[1] M. R. Schafroth, Phys. Rev. **100**, 463 (1955).
[2] H. Matsuda and T. Tsuneto, Suppl. Prog. Theor. Phys. **46**, 411 (1970).
[3] K. Liu and M. Fisher, J. Low Temp. Phys. **10**, 655 (1973).
[4] Kenn Kubo and Satoshi Takada, J. Phys. Soc. Jpn. **52**, 2108 (1983).
[5] R. Micnas, J. Ranninger, and S. Robaszkiewicz, Rev. Mod. Phys. **62**, 113 (1990).
[6] M. Greiner, O. Mandel, T. Esslinger, T. W. Hänsch, and I. Bloch, Nature (London) **415**, 39 (2002).
[7] O. Penrose and L. Onsager, Phys. Rev. **104**, 576 (1956).
[8] G. G. Batrouni and R. T. Scalettar, Phys. Rev. Lett. **84**, 1599 (2000).
[9] F. Hébert, G. G. Batrouni, R. T. Scalettar, G. Schmid, M. Troyer, and A. Dorneich, Phys. Rev. B **65**, 014513 (2001).
[10] Guido Schmid, Synge Todo, Matthias Troyer, and Ansgar Dorneich, Phys. Rev. Lett. **88**, 167208 (2002).
[11] V. J. Emery and S. A. Kivelson, Physica C **209**, 597 (1993); Nature (London) **374**, 434 (1995); Phys. Rev. Lett. **74**, 3253 (1995).
[12] Steven R. White and D. J. Scalapino, Phys. Rev. B **61**, 6320 (2001).
[13] R. T. Scalettar, G. G. Batrouni, A. P. Kampf, and G. T. Zimanyi, Phys. Rev. B **51**, 8467 (1995).
[14] C. Pich and E. Frey, Phys. Rev. B **57**, 13712 (1998).
[15] K. Bernardet, G. G. Batrouni, J.-L. Meunier, G. Schmid, M. Troyer, and A. Dorneich, Phys. Rev. B **65**, 104519 (2002).
[16] The antiferromagnetic domain texture appears as a result of the minimization of elastic and magnetoelastic energies.
[17] A. A. Belavin and A. M. Polyakov, JETP Lett. **22**, 245 (1975).
[18] F. Waldner, J. Magn. Magn. Mater. **54-57**, 837 (1986); Phys. Rev. Lett. **65**, 1519 (1990).
[19] S. I. Belov and B. I. Kochelaev, Solid State Commun. **103**, 249 (1997).
[20] Carsten Timm and K. H. Bennemann, Phys. Rev. Lett. **84**, 4994 (2000).
[21] T. Kamppeter, S. A. Leonel, F. G. Mertens, M. E. Gouvea, A. S. T. Pires, and A. S. Kovalev, Eur. Phys. J. B **21**, 93 (2001).
[22] Denis D. Sheka, Boris A. Ivanov, and G. Mertens, Phys. Rev. B **64**, 024432 (2001).
[23] R. A. Istomin and A. S. Moskvin, JETP Lett. **61**, 898 (2000).
[24] I. Kanazawa, Physica C **234-237**, 392 (2003).
[25] A. S. Ovchinnikov, I. G. Bostrem, and A. S. Moskvin, Phys. Rev. B **66**, 134304 (2002).
[26] A. S. Moskvin, I. G. Bostrem, and A. S. Ovchinnikov, JETP Lett. **78**, 772 (2003).
[27] Ar. Abanov and V. L. Pokrovsky, Phys. Rev. B **58**, R8889 (1998).
[28] A. G. Green, Phys. Rev. B **61**, R16299 (2000).
[29] Carsten Timm, S. M. Girvin, and H. A. Fertig, Phys. Rev. B **58**, 10634 (1998).
[30] S. A. Kivelson and B. Z. Spivak, Phys. Rev. B **45**, 10490 (1992).
[31] M. Rao, S. Sengupta, and R. Shankar, Phys. Rev. Lett. **79**, 3998 (1997).
[32] R. J. Gooding, Phys. Rev. Lett. **66**, 2266 (1991).
[33] A. L. Shluger and A. M. Stoneham, J. Phys.: Condens. Matter **5**, 3049 (1993).
[34] A. S. Moskvin and Yu. D. Panov, Phys. Rev. B **68**, 125109 (2003).
[35] A. S. Moskvin and A. S. Ovchinnikov, J. Magn. Magn. Mater. **186**, 288 (1998); Physica C **296**, 250 (1998).
[36] It is worth noting that in the frame of the BCS-like scenario, the symmetry of the order parameter is strictly defined in a momentum space, albeit the discussion of different experimental data has usually been performed with a real-space distributed order parameter.